Analytical Methods

Accepted Manuscript

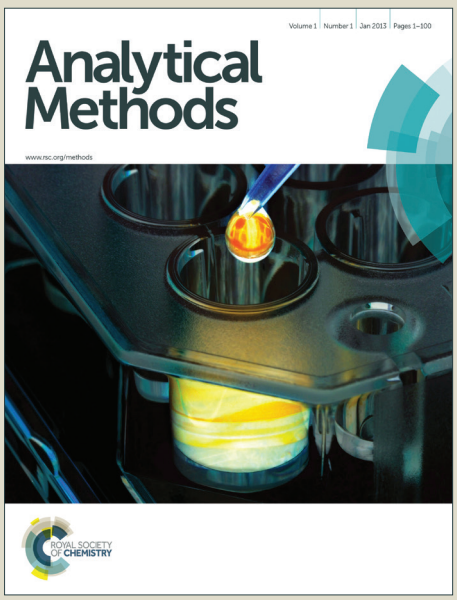

ROYAL SOCIETY OF CHEMISTRY

www.rsc.org/methods

The synthesis of novel Mn-doped CdTe fluorescence probes and their application in the determination of luteolin

Li Li[a], Lurong Yu[a], Yaping Ding*[a], Qiaolin Zhang[a], Yaxiang Lu[b]

[a]Department of Chemistry, Shanghai University, Shanghai, 200444, PR China

[b]School of Chemical Engineering, University of Birmingham, Birmingham, B15 2TT, UK

* *Corresponding author: Tel: +86-21-66134734, Fax: +86-21-66132797*
Address: Department of Chemistry, Shanghai University, Shanghai 200444, PR China

E-mail: wdingyp@sina.com

Abstract

In the present study, a novel and sensitive fluorescence probe method has been established for the determination of luteolin (LTL) based on the fluorescence quenching effect of LTL on glutathione (GSH)-capped Mn-doped CdTe quantum dots (QDs). GSH-capped Mn-doped CdTe QDs with a diameter of 6–8 nm were synthesized via a facile and inexpensive method in an aqueous system. The fluorescence of doped CdTe QDs at 541 nm was quenched in the presence of LTL with excitation wavelength at 351 nm and the fluorescence quenching efficiency is closely related to the amount of LTL added to the QDs solution, they present a linear relationship when the concentrations of LTL vary from 6 to 138 μM. The mechanism of the interaction between doped CdTe QDs and LTL was investigated and has been confirmed as dynamic quenching mechanism. The proposed method was successfully applied to the determination of LTL, and satisfactory results were obtained.

Keywords: Mn-doped CdTe, fluorescence probes, luteolin, determination

1. Introduction

Luteolin (LTL), a kind of natural plant extract, is an important member of the flavonoid family and is found in high amounts in peanut shells, celery, green pepper and chamomile tea[1]. Its molecular structure is given in Scheme 1. Researchers have found that LTL can exert various beneficial activities, among which cardiovascular protection, cataract prevention, anticancer and antiviral activity are the most important ones[2-4]. For example, Lee and co-workers[5] have found that LTL can effectively suppress the growth of MDA-MB-231 ER-negative breast cancer cell by means of inhibiting the survival of EGFR-mediated cell. In addition, a study has shown that LTL can be used in preparing alexin medicine for treating and preventing severe acute respiratory syndrome (SARS)[6]. Based on its wide and favorable applications, the research of convenient and reliable determination methods of LTL is significant and imperative.

Scheme. 1 here

Lots of methods have been reported for detecting the content of LTL, however, most such studies only focus on high performance liquid chromatography[7-9], capillary electrophoresis[10-12], spectrophotometric[13] and electrochemical methods[14-16]. Fluorimetry, as a method for the quantitative determination of certain significant ions or molecules such as Hg^{2+}[17]、Pb^{2+}[18] and ascorbic acid[19] has been gradually developed and captured much attention of investigators. Compared with the commonly used methods, fluorimetry has its own merits, such as simple experiment process, low reagent consumption, wide linear range, low detection limit, and satisfactory sensitivity.

Quantum dots (QDs), as a kind of inorganic semiconductor nanocrystals, have attracted considerable attention owing to their excellent optical properties. Among them, doped QDs have been attained more widely research as the incorporation of impurities could offer QDs innovative

remarkable optical properties compared to that of the undoped ones, including higher fluorescence efficiency, better photochemical stability, longer lifetime, more effective photo-oxidation protection[20], etc. Therefore, doped QDs could serve as ideal fluorescence probes for the determination of multifarious ions or molecules. For instance, Mn-doped ZnS has been used for detection of Co^{2+} [21], glucose[22] and sudan dyes in foodstuffs[23]; Mn-doped CdTe has been applied in determination of human IgG[24], ascorbic acid[25] and so on. In addition, in order to achieve water solubility and stabilization, the surfaces of QDs need to be modified by stabilizing agents. Some organic ligands such as mercaptoacetic acid[26], mercaptopropionic acid[27], cysteine[28], 2-mercaptoethanol[29] and glutathione (GSH)[30] are frequently used for QDs modification. Studies have indicated that the GSH-capped QDs possess high fluorescence quantum yield, narrow emission spectra, satisfactory biocompatibility and less toxicity. Therefore, the GSH-capped Mn-doped CdTe QDs could act as efficient fluorescence probes in the analytical field.

To the best of our knowledge, the utilization of GSH-capped Mn-doped CdTe QDs as fluorescence probe for the quantitative determination of LTL has not been reported so far. Herein, in this study, we employed a straightforward process to synthesize the GSH-capped Mn-doped CdTe QDs by using inorganic salts as precursors and GSH as the stabilizer. The as-prepared QDs were used for the determination of LTL. Under optimum conditions, a novel analytical method for the determination of LTL with high sensitivity was established.

2 Experimental section

2.1 Reagents

Sodium borohydride ($NaBH_4$), tellurium powder (Te), cadmium chloride ($CdCl_2 \cdot 2.5H_2O$), manganese chloride ($MnCl_2 \cdot 4H_2O$), glutathione (GSH), luteolin (LTL) and other routine chemicals

were all analytical grade and used without further purification. All of them were purchased from Shanghai Sinopharm Chemical Reagent Co. Ltd. (China). Duyiwei capsules were purchased from the local drugstore. Deionized water was used throughout the experiment. The phosphate buffer solution was prepared by adjusting 0.1 M K_2HPO_4, KH_2PO_4, H_3PO_4, or NaOH, accordingly.

2.2 Apparatus

X-ray powder diffraction (XRD) spectra were obtained from a Haoyuan DX-2700 X-ray diffractometer (China). Transmission electron microscopy (TEM) images were acquired using a JEOL-200 CX transmission electron microscope (Japan). An AVATAR 370 Fourier transform infrared (FTIR) spectrophotometer (America) was utilized to record the FTIR spectra. An UV-2501PC spectrometer (Shimadzu, Japan) was applied to record the ultraviolet visible (UV-Vis) absorption spectrum. The fluorescence emission spectra were recorded via a RF-5301PC spectrofluorophotometer (Shimadzu, Japan). A pHS-3C pH meter (Analytical Instruments Co., Shanghai, China) was utilized to measure the pH values of the aqueous solutions.

2.3 Synthesis methods

2.3.1 Synthesis of NaHTe precursor solution

The solution of NaHTe was prepared according to a previously reported literature[31]. $NaBH_4$ solution was prepared and degassed with nitrogen for 7 min. After that, Te powder was injected into the oxygen-free solution. The molar ratio of Te and $NaBH_4$ was 1:20. As the generation of H_2 during the process was occurred, a small outlet linked to the small flask was used to release the pressure. When the color of solution changed back to colorless and Te powder was completely reacted, it means the NaHTe solution was obtained.

2.3.2 Synthesis of GSH-capped Mn-doped CdTe QDs

The QDs were prepared based on a reported literature with some modifications[32]. In this work, the molar ratio of Cd^{2+} / Te^{2-} / GSH was fixed to be 2:1:2.4 and the Mn^{2+} content was 5% of cadmium. Briefly, 45.67 mg $CdCl_2 \cdot 2.5H_2O$ and 147.5 mg GSH was added into a three-necked round-bottomed flask and dissolved in 180 ml double distilled water. After dissolved completely and stirred uniformly, 500 μL 0.02 M $MnCl_2 \cdot 4H_2O$ was added. Then, the pH of the mixed solution was adjusted to 9 with 1 M NaOH solution which was added dropwise until the mixture changed from ivory to clear. Subsequently, the dissolved oxygen was driven off by nitrogen with a medium velocity for about 30 min. Then, the oxygen-free NaHTe precursor solution was injected quickly into the above solution under vigorous stirring. The color of the solution changed immediately to orange and CdTe QDs core were formed in this stage. After that, the resulting solution was heated to boil for 10 min under refluxed condition for the further growth of cores. In order to obtain Mn-doped CdTe QDs with less surface defects, the solution was transferred to a water bath refluxed at 60℃ for 1 hour. Finally, the salmon pink GSH-capped Mn-doped CdTe QDs were obtained.

After the preparation of GSH-capped Mn-doped CdTe QDs stock solution, the same volume of ethanol was added for the precipitation of QDs, supporting for the further characterization like XRD and FTIR analysis.

3 Results and discussion

3.1 Characterization of the prepared QDs

The structures of GSH-capped Mn-doped CdTe QDs and GSH-capped CdTe QDs were obtained through the XRD analysis, as shown in Fig. 1. The two broad and distinct diffractive peaks correspond respectively to the crystal planes [002] and [103], confirming that they are hexagonal crystalline structure. Intuitively, the two XRD patterns have no obvious difference, we can't find obvious

diffraction peak of Mn from the XRD pattern of Mn-doped CdTe QDs due to the successfully trace doping of Mn^{2+} ions occupied the lattice site and replaced some Cd^{2+} ions. The particles have an average diameter of 7.56 nm determined by Scherrer equation: $D = K\lambda / (\beta \cos\theta)$, where D is the grain size, K is Scherrer constant, λ is the wavelength of X-ray radiation, β is the full width at half maximum, and θ is the diffraction angle.

Fig. 1 here

The morphology of GSH-capped Mn-doped CdTe QDs was investigated by TEM, as depicted in Fig. 2. We can observe that the dispersion of QDs seems not very well, it appears some aggregation. This is owing to the property of nanoparticles which are easy to reunite together. However, it still can observe clearly that the QDs are spherical and their uniform particle sizes are about 7 nm, which is consistent with the size estimated by the Scherrer formula calculations based on the XRD pattern.

Fig. 2 here

In order to identify the successful conjugation between GSH and Mn-doped CdTe QDs, FTIR spectra of pure GSH and the GSH-capped Mn-doped CdTe QDs were recorded and shown in Fig. 3. We can note that the distinct difference between the two spectra is at 2524 cm^{-1}, which belongs to the S-H stretching vibration characteristic absorption. Nevertheless, this characteristic absorption band disappeared in the FTIR spectrum of GSH-capped Mn-doped CdTe QDs, indicating the formation of Cd-S coordination bond, which means the successful conjugation of GSH molecules and Mn-doped CdTe QDs by thiol bond.

Fig. 3 here

3.2 The optical properties of GSH-capped Mn-doped CdTe QDs

QDs have excellent optical properties compared with traditional organic fluorescent dyes. In

general, UV-Vis and fluorescence spectra are usually used to describe the optical properties of QDs. As shown in Fig. 4, the synthesized QDs have a wide UV-Vis absorption wavelength; meanwhile, their fluorescence spectrum is narrow and symmetrical with the maximum emission peak around 541 nm when the excitation wavelength is 351 nm, which is favorable for its application in analysis.

Fig. 4 here

The quantum yield (QY) of GSH-capped Mn-doped CdTe QDs was calculated to be 48% according to the standard expression formula of *QY*: $QY_u = QY_s (F_u A_s n_u^2) / (F_s A_u n_s^2)$, the subscripts "*u*" and "*s*" denote sample and standard. *QY* is the fluorescence quantum yield. *A* is absorption values at excitation wavelength, *F* is the integrated fluorescence intensity, and *n* is the refractive index of solvent. In the present study, sample is the synthesized GSH-capped Mn-doped CdTe QDs, standard is rhodamine B. The solvent used in this experiment is water, and its refractive index is 1.333 at room temperature. The fluorescence quantum yield of rhodamine B in water is reported to be 31%.

Furthermore, a comparison was made about the fluorescence intensity of GSH-capped Mn-doped CdTe QDs and GSH-capped CdTe QDs to explore the effect of Mn impurity. The result shown in Fig. 5 demonstrates that the Mn-doped QDs have a higher fluorescence intensity compared with the ones without Mn.

Fig. 5 here

3.3 Optimization of determination conditions

3.3.1 Effect of incubation time

The effect of incubation time on the fluorescence intensity of aqueous GSH-capped Mn-doped CdTe QDs-LTL solution system was investigated and the result is shown in Fig. 6. From the figure we can see that within the initial reaction time about one and a half hour, the fluorescence intensity of the

reaction system is not stable. After that, the fluorescence intensity gradually stabilized with a slight decline when time extended beyond 3 hours which is due to the partly oxidized of QDs. Therefore, we choose 90 min as the optimal incubation time. Compared to that of other detection methods, the incubation time is a little longer on account of the steric hindrance effect of GSH. However, it doesn't do obvious effect to the result of detection.

Fig. 6 here

3.3.2 Effect of pH

In order to investigate the influence of pH on the fluorescence intensity of our system, we employed the 0.1 M phosphate buffer solution with pH ranging from 6 to 11 as solvent, and the result is shown in Fig. 7. In the zone of acidic to neutral, the fluorescence intensity of reaction system is extremely lower due to the protonation of sulfhydryl that break away from the surface of QDs, which lead to the appearance of some defects on the surface of QDs. When the pH of system changed from 9 to 10, the fluorescence intensity reached to the highest and maintained stable. However, with the increase of alkalinity, a sharp drop of the fluorescence intensity occurred, which may be attributed to the formation of $Cd(OH)_2$ precipitation. Thus, pH of 9.0 was selected for further experiments.

Fig. 7 here

3.4 Detection of LTL by quenching the fluorescence intensity of GSH-capped Mn-doped CdTe QDs

In order to measure the effect of LTL on the fluorescence of GSH-capped Mn-doped CdTe QDs, we prepared solutions with different amounts of LTL as follows. Firstly, 300 μL of GSH-capped Mn-doped CdTe QDs stock solution and different amounts of fresh LTL standard solutions were added into a series of 25 mL volumetric flasks, and then diluted the solutions with 0.1 M phosphate buffer

solution and mixed thoroughly for the further measurement. The fluorescent intensity of the above solutions were recorded at excitation wavelength of 351 nm and the slit widths used for excitation and emission were 5 nm respectively.

The investigation of the change of GSH-capped Mn-doped CdTe QDs fluorescence intensity with different amounts of LTL was conducted and the result is revealed in Fig. 8. It is obvious that with the increase of LTL concentration from 0 to 138 μM, the fluorescence intensity of QDs progressively decreased, which indicates that LTL could quench the fluorescence of QDs. Furthermore, the fluorescence quenching is closely related to the amount of LTL added to the QDs solution, based on which an analytical method can be established for the quantitative analysis of LTL. The quenching efficiency is proportional to the concentration of LTL from 6 to 138 μM, which can be described by the following equation: $log\ (F_0/F) = 0.01379C - 0.0520$ (C: μM), and the correlation coefficient (R) is equal to 0.9977, as shown in Fig. 9. Where F_0 and F are the fluorescence intensities of QDs in the absence and presence of LTL respectively, and C is the concentration of LTL.

Fig. 8 here

Fig. 9 here

The detection limit of LTL was calculated to be 61 nM based on the formula: $LOD = 3\sigma / k$, where σ is the standard deviation of the blank measurements and k is the slope of the calibration graph. Compared with other fluorescence probe methods reported to detect LTL, the method we established here has a wide linear range and an appropriate detection limit, the results are shown in Table 1.

Table 1 here

4 The possible quenching mechanism

There are many fluorescence quenching mechanisms which include Förster resonance energy transfer (FRET), static quenching, dynamic quenching, and electron transfer[35]. A possible quenching mechanism of our reaction system was investigated and proposed.

It is known that FRET can be occurred only when the emission spectrum of one fluorescent group overlapped with the absorption spectrum of another to a certain extent, and the distance between the two fluorescent groups (generally less than 100 Å) must be appropriate at the same time. However, there is little overlap between the UV-Vis absorption spectrum of LTL and the emission spectrum of the GSH-capped Mn-doped CdTe QDs, as shown in Fig. 10. Therefore, the fluorescence quenching of GSH-capped Mn-doped CdTe QDs by LTL is not caused by FRET.

Fig. 10 here

We continue to study the possibility of dynamic and static quenching mechanism in the following part. The quenching behavior of low concentration of LTL on the fluorescence of synthesized QDs can be illustrated by the well-known Stern–Volmer equation[36]: $F_0 / F = K [Q] + 1$, where F_0 and F are the fluorescence intensities in the absence and presence of quencher (LTL) respectively. $[Q]$ is the concentration of the quencher. k is the Stern–Volmer quenching constant, which defines the quenching efficiency of the quencher.

Dynamic quenching is associated with molecular collision. The rise of temperature will lead to the increase of molecular collision probability, thus increasing the non-radiative transition of excited state molecules, which increased the quenching constant. On the contrary, the increased temperature may reduce the stability of complexes, thereby reducing the quenching constant. Therefore, we have investigated the change of relative fluorescence intensity with the increasing concentration under different temperatures. The results displayed in Fig. 11. Quenching constants of the QDs–LTL solution

system at three different temperatures were calculated according to the Stern–Volmer equation, which are listed in Table 2. It can be seen that the quenching constants increased with the rise of temperature, which indicates that the quenching type of the GSH-capped Mn-doped CdTe QDs–LTL reaction system is dynamic quenching.

Fig. 11 here

Table 2 here

In order to confirm the dynamic quenching mechanism, the absorption spectra of related solutions were measured. As is known, in dynamic quenching, the fluorescence is quenched when the quencher collides with the excited fluorescent molecule. In other words, collision quenching affects only the excited state of fluorescent molecular, and no changes in the absorption spectrum. Nevertheless, the formation of ground-state complex in static quenching will perturb the absorption spectrum of the fluorescent molecule. Hence, the UV-Vis absorption spectra were investigated to distinguish the dynamic and static quenching mechanism. The absorption spectra of GSH-capped Mn-doped CdTe QDs (a), mixture of QDs and LTL (b), LTL (phosphate buffer solution as the reference) (c) , and LTL (QDs as the reference) (d) are shown in Fig. 12. Obviously, we can see that curve (b) is a simple superposition of curve (a) and curve (c), and curve (c) and (d) are almost entirely overlapped with each other. These suggest that the absorption spectrum of the mixture of QDs and LTL is a linear combination of the spectra of each component. That is to say, the absorption spectra have no change which confirmed that the quenching mechanism is dynamic quenching.

Fig. 12 here

As is known, when dynamic quenching occurs, the lifetime of the fluorescence system will shorten. However, when static quenching occurs, the lifetime will remain constant. In order to confirm

the dynamic quenching mechanism further, we have measured the fluorescence lifetime of GSH-capped Mn-doped CdTe QDs in the absence and presence of LTL. The values are listed in Table 3. Monoexponential decay is inadequate, so two exponentials are used to describe the data. The average lifetime is calculated by the following equation: $\tau = A_1 \tau_1 + A_2 \tau_2$, where τ is the average lifetime, τ_1 and τ_2 are the lifetime of fast and slow decays, respectively. A_1 and A_2 are the weights of each process.

Table 3 here

The average lifetime was measured to be 31.69 ns in the absence of LTL. When the LTL added, the lifetime of QDs decreased to be 28.82 ns. This situation further confirmed a dynamic quenching mechanism.

5 Selectivity and analytical applications

5.1 Selectivity

Many compounds which are usually contained in pharmaceutical preparation have the potency to quench QDs fluorescent intensity as well. In order to investigate the practical application possibility of the developed method to determinate LTL, the interference of some familiar foreign substances were tested under the optimum conditions. From the results displayed in Table 4, it is clearly to see that most of the glucide, amino acids and common metal ions could be coexist with LTL at high concentration, whereas Mg^{2+} and Ca^{2+} could be tolerate at lower concentration levels.

Table 4 here

5.2 Analytical application

The practical feasibility of the proposed method was evaluated by determining LTL in commercial Duyiwei capsules. The recovery and relative standard deviation (RSD) were tested through the standard addition method, and the results are shown in Table 5. The recovery and RSD of the samples were

generally satisfactory and can meet the requirements of actual analysis.

Table 5 here

6 Conclusions

In this article, a novel and convenient method for the determination of LTL has been established. GSH-capped Mn-doped CdTe QDs were obtained through the simple and inexpensive hydrothermal synthesis method. LTL could quench the fluorescence of as-prepared QDs, and the fluorescence quenching is closely related to the amount of LTL. Under the optimum conditions, a good linear relationship between fluorescence intensity of the system and the concentration of LTL in the range of 6 to 138 μM could be achieved, and the limit of detection is 61 nM. Possible quenching mechanism between LTL and GSH-capped Mn-doped CdTe QDs is also discussed which has been identified as dynamic quenching mechanism.

Acknowledgments

This research is supported by the National Natural Science Foundation of China (NSFC) (No. 21271127, 61171033), the Nano-Foundation of Science and Techniques Commission of Shanghai Municipality (No. 12nm0504200) and the Natural Science Foundation of Shanghai Municipality (No. 13ZR1415600).

References

1. A. C. Franzoi, I. C. Vieira, J. Dupont, C. W. Scheeren and L. F. de Oliveira, *Analyst*, 2009, 134, 2320-2328.
2. M. Funakoshi-Tago, K. Nakamura, K. Tago, T. Mashino and T. Kasahara, *Int Immunopharmacol*, 2011, 11, 1150-1159.
3. Y. S. Lang, D. Chen, D. Y. Li, M. Y. Zhu, T. D. Xu, T. Zhang, W. H. Qian and Y. Y. Luo, *J Pharm Pharmacol*, 2012, 64, 597-603.
4. R. X. Shi, Q. Huang, X. Q. Zhu, Y. B. Ong, B. Zhao, J. Lu, C. N. Ong and H. M. Shen, *Mol Cancer Ther*, 2007, 6, 1338-1347.
5. E. J. Lee, S. Y. Oh and M. K. Sung, *Food Chem Toxicol*, 2012, 50, 4136-4143.
6. T. Zhang and D. F. Chen, *J Ethnopharmacol*, 2008, 117, 351-361.

7. L. P. Li and H. D. Jiang, *J Pharmaceut Biomed*, 2006, 41, 261-265.
8. F. Fang, J. M. Li, Q. H. Pan and W. D. Huang, *Food Chem*, 2007, 101, 428-433.
9. Y. M. Sun, H. L. Wu, J. Y. Wang, Z. Liu, M. Zhai and R. Q. Yu, *J Chromatogr B*, 2014, 962, 59-67.
10. X. Q. Xu, L. S. Yu and G. N. Chen, *J Pharmaceut Biomed*, 2006, 41, 493-499.
11. S. Zhang, S. Q. Dong, L. Z. Chi, P. G. He, Q. J. Wang and Y. Z. Fang, *Talanta*, 2008, 76, 780-784.
12. S. J. Sheng, L. Y. Zhang and G. Chen, *Food Chem*, 2014, 145, 555-561.
13. R. Cai, S. S. Wang, Y. Meng, Q. G. Meng and W. J. Zhao, *Anal Methods-Uk*, 2012, 4, 2388-2395.
14. L. J. Zeng, Y. F. Zhang, H. Wang and L. P. Guo, *Anal Methods-Uk*, 2013, 5, 3365-3370.
15. A. Y. Tesio, A. M. Granero, N. R. Vettorazzi, N. F. Ferreyra, G. A. Rivas, H. Fernandez and M. A. Zon, *Microchem J*, 2014, 115, 100-105.
16. P. F. Pang, Y. P. Liu, Y. L. Zhang, Y. T. Gao and Q. F. Hu, *Sensor Actuat B-Chem*, 2014, 194, 397-403.
17. L. L. Li, G. H. Wu, T. Hong, Z. Y. Yin, D. Sun, E. S. Abdel-Halim and J. F. Zhu, *Acs Appl Mater Inter*, 2014, 6, 2858-2864.
18. S. Y. Liu, W. D. Na, S. Pang and X. G. Su, *Biosens Bioelectron*, 2014, 58, 17-21.
19. M. B. Lima, S. I. E. Andrade, I. S. Barreto and M. C. U. Araujo, *Food Anal Method*, 2014, 7, 1598-1603.
20. N. Pradhan and X. G. Peng, *J Am Chem Soc*, 2007, 129, 3339-3347.
21. W. Bian, J. Ma, Q. L. Liu, Y. L. Wei, Y. F. Li, C. Dong and S. M. Shuang, *Luminescence*, 2014, 29, 151-157.
22. M. Sharma, T. Jain, S. Singh and O. P. Pandey, *Aip Adv*, 2012, 2.
23. M. Zhou, X. F. Chen, Y. Y. Xu, J. C. Qu, L. X. Jiao, H. G. Zhang, H. L. Chen and X. G. Chen, *Dyes Pigments*, 2013, 99, 120-126.
24. G. X. Liang, H. C. Pan, Y. Li, L. P. Jiang, J. R. Zhang and J. J. Zhu, *Biosens Bioelectron*, 2009, 24, 3693-3697.
25. L. Li, X. Y. Cai, Y. P. Ding, S. Q. Gu and Q. L. Zhang, *Anal Methods-Uk*, 2013, 5, 6748-6754.
26. Z. Chen, J. Y. Chen, Q. W. Liang, D. D. Wu, Y. E. Zeng and B. Jiang, *J Lumin*, 2014, 145, 569-574.
27. Y. Q. Cao, N. Liu, P. Yang, Y. N. Zhu, R. X. Shi, Q. Ma and A. Y. Zhang, *J Nanosci Nanotechno*, 2014, 14, 5238-5243.
28. L. Feng, H. Y. Kuang, X. Y. Yuan, H. W. Huang, S. J. Yi, T. L. Wang, K. Q. Deng, C. R. Tang and Y. L. Zeng, *Spectrochim Acta A*, 2014, 123, 298-302.
29. W. E. Mahmoud, *Sensor Actuat B-Chem*, 2012, 164, 76-81.
30. Y. Z. Shen, S. P. Liu, J. D. Yang, L. L. Wang, X. P. Tan and Y. Q. He, *Sensor Actuat B-Chem*, 2014, 199, 389-397.
31. Y. H. Zhang, H. S. Zhang, M. Ma, X. F. Guo and H. Wang, *Appl Surf Sci*, 2009, 255, 4747-4753.
32. L. J. Zhang, C. L. Xu and B. X. Li, *Microchim Acta*, 2009, 166, 61-68.
33. Y. Z. Shen, S. P. Liu, Z. Q. Liu and Y. Q. He, *Spectrosc Lett*, 2013, 46, 483-492.
34. B. W. Xiao, H. J. Wang, X. J. Zhao and Y. F. Li, *Anal Methods-Uk*, 2014, 6, 2894-2899.
35. J. J. Peng, S. P. Liu, S. G. Yan, X. Q. Fan and Y. Q. He, *Colloid Surface A*, 2010, 359, 13-17.

36. W. J. Jin, J. M. Costa-Fernandez, R. Pereiro and A. Sanz-Medel, *Anal Chim Acta*, 2004, 522, 1-8.

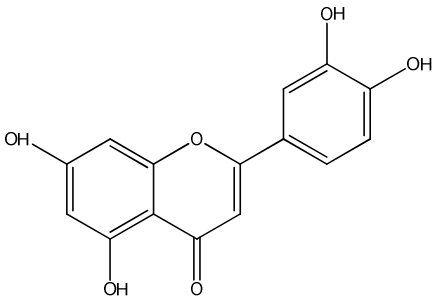

Scheme. 1 Molecular structure of LTL.

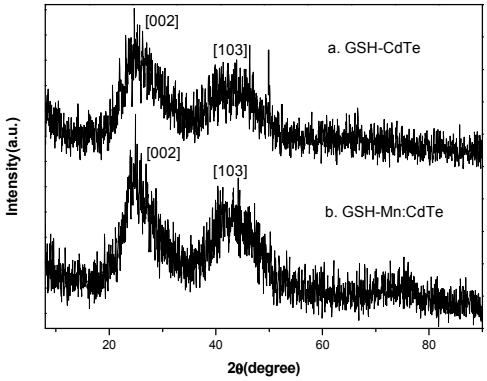

Fig. 1 XRD patterns of GSH-capped CdTe QDs and GSH-capped Mn-doped CdTe QDs.

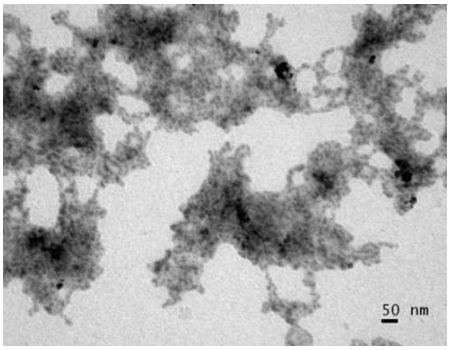

Fig. 2 TEM image of GSH-capped Mn-doped CdTe QDs.

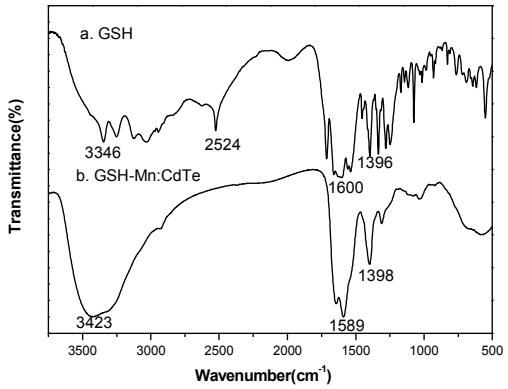

Fig. 3 FTIR spectra of GSH and GSH-capped Mn-doped CdTe QDs.

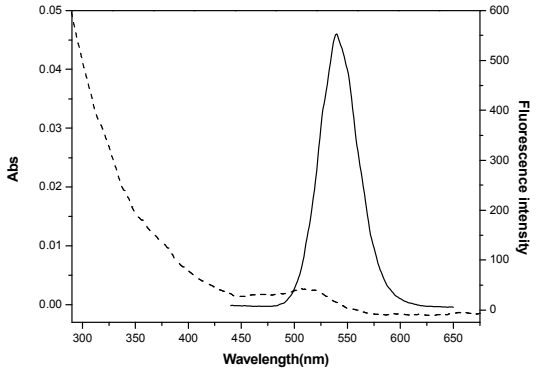

Fig. 4 UV-Vis absorption spectrum (dash line) and fluorescence emission spectrum (solid line) of GSH-capped Mn-doped CdTe QDs (C_{QDs} = 0.167 μM, λex = 351 nm).

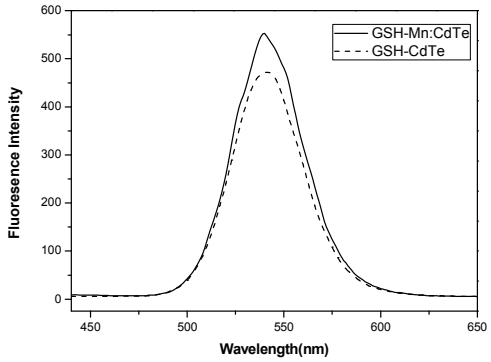

Fig. 5 Fluorescence emission spectra of GSH-capped CdTe QDs (C_{QDs} = 0.167 μM) and GSH-capped Mn-doped CdTe QDs (C_{QDs} = 0.167 μM) at the excitation wavelength of 351 nm.

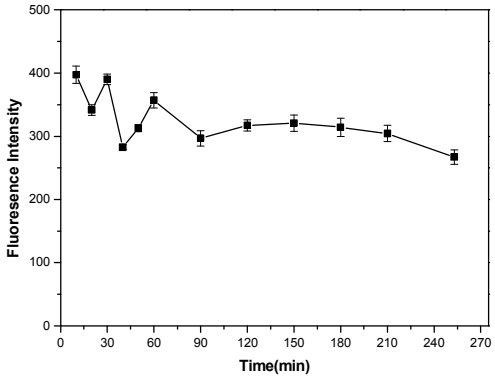

Fig. 6 Effect of incubation time on the fluorescence intensity of GSH-capped Mn-doped CdTe QDs-LTL solution system (C_{QDs} = 0.167 μM, C_{LTL} = 24 μM).

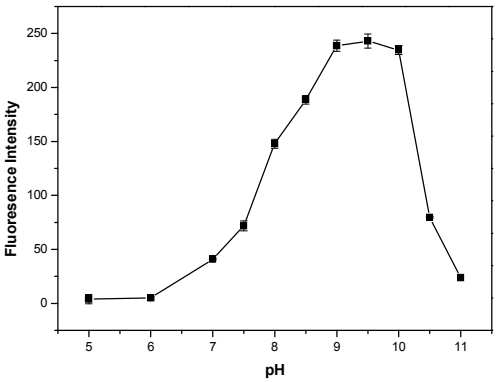

Fig. 7 Effect of pH on the fluorescence intensity of GSH-capped Mn-doped CdTe QDs (C_{QDs} = 0.167 μM) in the presence of LTL (C_{LTL} = 24 μM).

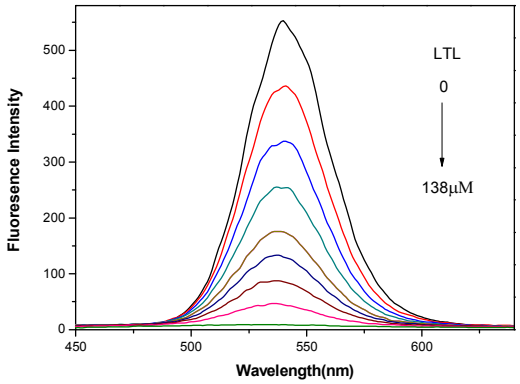

Fig. 8 Fluorescence emission spectra of GSH-capped Mn-doped CdTe QDs (C_{QDs} = 0.167 μM) in the presence of LTL at various concentrations in 0.1 M phosphate buffer solution at pH 9. The LTL was added to yield final concentrations of 0, 16, 22, 34, 46, 52, 58, 76, 138 μM.

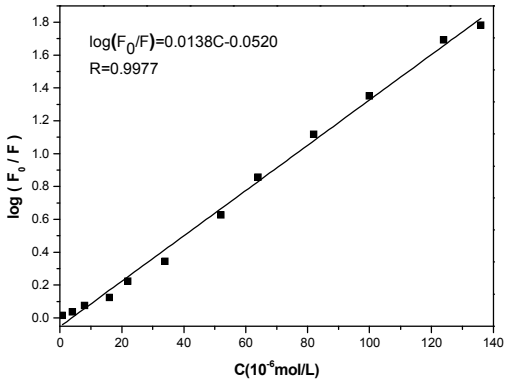

Fig. 9 Linear curve of the logarithm of relative fluorescence intensity log (F_0/F) versus the concentration (C) of LTL.

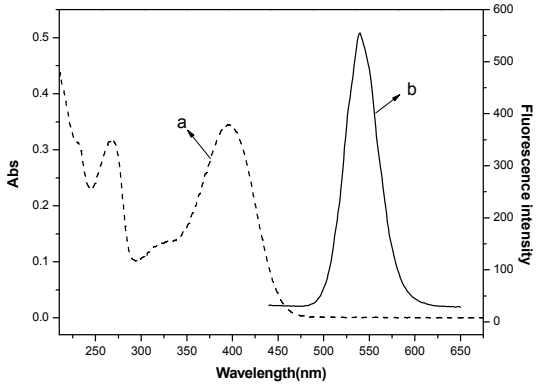

Fig. 10 UV-Vis absorption spectrum of LTL (C_{LTL} = 14 μM) (a) and fluorescence spectrum of GSH-capped Mn-doped CdTe QDs (C_{QDs} = 0.167 μM) (b).

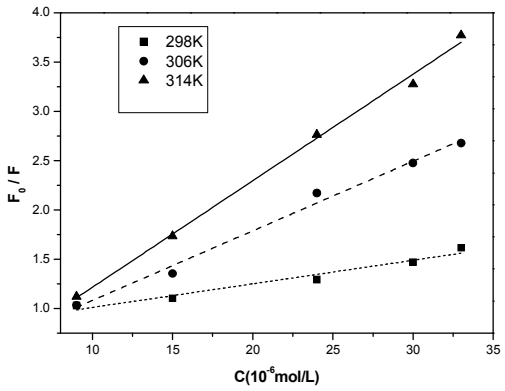

Fig. 11 Stern–Volmer plots for the QDs–LTL solution system (C_{QDs} = 0.167 μM) at three different temperatures, 298k, 306k, 314k, respectively, in 0.1 M phosphate buffer solution at pH 9.

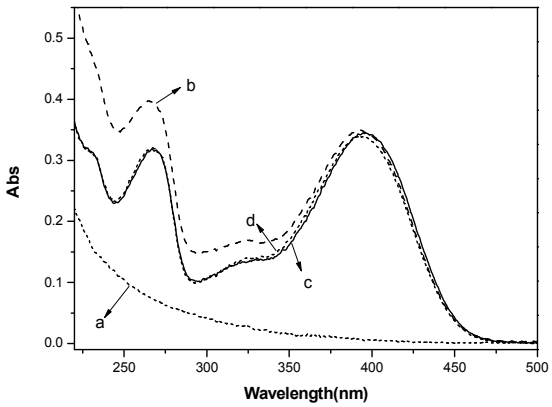

Fig. 12 UV–Vis absorption spectra of GSH-capped Mn-doped CdTe QDs (a), mixture of QDs and LTL (b), LTL (phosphate buffer solution as the reference, pH 9) (c), and LTL (QDs as the reference) (d) (C_{QDs} = 0.167 μM, C_{LTL} = 14 μM).

Table 1 Comparison of the fluorescent sensors for the determination of LTL

Method	Calibration range (10^{-6}M)	Detection limit (M)	Reference
TGA-capped CdTe/CdS QDs	1 - 69.9	3.5×10^{-9}	33
LTL-Zn^{2+} complex	1.2 - 23.1	6.4×10^{-7}	34
GSH-capped Mn-doped CdTe QDs	6-138	6.1×10^{-8}	Present method

Table 2 Parameters of Stern–Volmer plots of QD–LTL solution system

Temperature (K)	Sterm–Volmer linear equation	K ($L\cdot mol^{-1}$)	R
298	F_0/F=0.0239C+0.7711	0.0239	0.9745
306	F_0/F=0.0707C+0.3739	0.0707	0.9940
314	F_0/F=0.1081C+0.1345	0.1081	0.9976

Table 3 Fluorescence lifetime of the GSH-capped Mn-doped CdTe QDs (C_{QDs} = 0.001 M) in the absence and presence of LTL (C_{LTL} = 10^{-5} M).

C_{LTL} (10^{-5} M)	Lifetime (ns)		Amplitude (%)		τ
	τ_1	τ_2	A_1	A_2	
0	16.55	41.87	40.20	59.80	31.69
18	16.07	41.40	49.68	50.32	28.82

Table 4 Effect of potentially interfering species (C_{LTL}=32μM)

Coexisting substances	Concentration （μM）	Relative error (%)	Coexisting substances	Concentration （μM）	Relative error (%)
Glucose	480	3.716	Na^+, I^-	4800	-3.463
Maltose	640	1.952	Na^+, Cl^-	2560	-4.689
Sucrose	640	-0.939	Caffeine	160	-4.902
Mg^{2+}, SO_4^{2-}	96	4.160	Glycine	4800	-5.507
Ca^{2+}, Cl^-	96	0.354	L-Arginine	480	-3.326
Zn^{2+}, SO_4^{2-}	160	-2.199	L- Alanine	320	2.448
K^+, NO_3^-	1920	-3.192	L-Tryptophan	960	2.205
NH^{4+}, Cl^-	1920	-4.960			

Table 5 Results of Duyiwei capsule sample analysis

Number	Found (μM)	Standard added (μM)	Found after addition (μM)	Average recovery(%)	RSD (%)
1	18.05	26	43.61	98.35	2.80
2	24.47	28	52.70	100.82	3.13
3	28.38	30	59.14	102.52	3.45

Graphical Abstract

Mn-doped CdTe QDs were prepared. Luteolin can reduce its fluorescence intensity, based on which to realize the detection of luteolin.